Multiple Impedance Control for Object Manipulation

S. Ali A. Moosavian[1] and Evangelos Papadopoulos[2]

[1]Department of Mechanical Engineering, K. N. Toossi University of Technology, PO Box 16765-3381, Tehran, Iran

[2]Department of Mechanical Engineering, National Technical University of Athens, 15773 Zografou, Greece

Abstract

Impedance Control was formulated originally to impose a desired behavior on a single manipulator interacting with its environment. In this paper, a new algorithm called Multiple Impedance Control (MIC) is proposed for the cooperative manipulation of a common object. The general formulation for the MIC algorithm is developed and is shown that under the MIC law all cooperating manipulators, and the manipulated object exhibit the same designated impedance behavior. At the same time, the potentially large object inertia and other forces are taken into account. An estimation procedure for contact force determination is given which results in a good approximation, even during an impact. Using an example, the response of the MIC algorithm is compared to that of the Object Impedance Control (OIC). It is shown that in the presence of flexibility, the MIC algorithm results in an improved performance.

I. Introduction

The control of mechanical manipulators is a challenging task, in part due to the strong nonlinearities in the equations of motion. To control the interaction forces or the dynamic behavior of the manipulator during tasks involving contact, force and impedance control laws have been proposed. A Hybrid Position/Force Algorithm has been suggested to control end-effector position in some directions, and contact forces in the remaining directions [1]. The Operational Space Formulation presents a control architecture with slow computation of dynamics, and a fast servo level to compute the control command [2, 3]. The mechanics of coordinative object manipulation by multiple robotic arms, taking the object dynamics into consideration, has been discussed in [4].

For a single manipulator in dynamic interaction with its environment, Impedance Control has been proposed that regulates the relationship between end-effector position and force [5]. An implementation of a combined impedance and force control has been also proposed to exert a desired force on the environment, and at the same time result in a desired relationship between this force and the relative location of the point of interaction (contact) with respect to the commanded manipulator location [6]. Planning issues for compliant motions have been studied in [7]. Adaptive schemes aiming at making impedance control capable of tracking a desired contact force, a main shortcoming of impedance control in the presence of an unknown environment, have been proposed [8]. The Object Impedance Control (OIC), an extension of impedance control, has been developed for multiple robotic arms manipulating a common object [9]. The OIC enforces a designated impedance not of an individual manipulator end-point, but of the manipulated object itself. A combination of feedforward and feedback controls is employed to make the object behave like a reference impedance. It has been realized that applying the OIC to manipulation of a flexible object may lead to instability [10]. Based on the analysis of a representative system, it was suggested that in order to solve the instability problem, one should either increase the desired mass parameters or filter and lower the frequency content of the estimated contact force.

The *Multiple Impedance Control* (MIC) was newly presented and applied to space free-flying multi-arm robotic systems [11]. In this article, the new MIC algorithm is developed for distinct cooperating manipulators, and important issues are detailed. The MIC enforces a reference impedance on both the manipulator end-points, and the manipulated object. Physically speaking, this means that both manipulator end-effectors and the object are controlled to behave like a designated impedance in reaction to any disturbing external force on the object, and hence, an accordant motion of the manipulators and payload is achieved. First, the basic concepts are introduced. Then, the general formulation for the MIC algorithm is presented, and the resulting tracking errors are studied. In addition, an estimation procedure is given for contact force determination. Finally, a simple model of a robotic arm manipulating an object is used to compare the performance of the MIC and OIC algorithms.

II. Definitions and Basic Concepts

A *manipulation task* is defined here as moving an object according to a predefined trajectory which may pass through an obstacle. To compare alternative control strategies in a manipulation task, the problem is considered first in a simple form. Figure 1 depicts a simplified model of a manipulation task performed by a single manipulator. In the case of a *cooperative* operation, this model can be completed by adding a cooperation strategy.

Considering Figure 1, the task is defined as moving the object m_3 according to a given trajectory, x_{3des}, by applying an appropriate force F_1 without any damaging impacts.

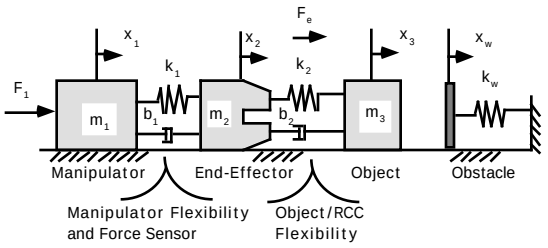

Fig. 1: Manipulation task by a simple robot.

The manipulator is represented by m_1 connected through a spring-damper to m_2 which represents the end-effector. A conceptual comparative analysis between existing control strategies, showed that use of a standard impedance law does not provide compensation for the object's inertia forces and yields unacceptable results when the object is massive, or when it experiences large accelerations [12]. Furthermore, even for a negligible object inertia, since this law enforces a relationship between x_2 (or $\dot{x}_2$) and F_e (with no feedback from the object motion), good tracking for x_3 is not guaranteed. On the other hand, the OIC which implements the impedance law at the object level, results in poor tracking in the presence of flexibility in the system. The more flexible the system is, the worse the performance of OIC will be. Some attempts to alleviate this problem by controller tuning were reported in [10].

III. Multiple Impedance Control Law

The strategy in Multiple Impedance Control (MIC) is to enforce an equivalent impedance relationship at the manipulator end-effector(s) level, *and* at the manipulated object level. Therefore, object inertia effects are compensated for in the impedance law, and at the same time, the end-effector(s) tracking errors are controlled. This means both the manipulator end-effector(s) and the manipulated object are controlled to respond as a designated impedance in reaction to any disturbing external force on the object. For mobile manipulators, e.g. space free-flyers, the MIC algorithm can be applied so that all participating manipulators, the free-flying spacecraft (base), and the manipulated object exhibit the same impedance behavior, as implied by "multiple" in the MIC name [12]. In this section, after a brief review on manipulator dynamics and object equations of motion, the MIC law is presented. Then, the tracking errors and an estimation procedure for contact force determination are studied.

(a) System Dynamics Modelling. Performing a cooperative manipulation task requires coordination between participating robotic arms, see Figure 2. To this end, the dynamics equations of each participating manipulator in the task space can be obtained as

$$\tilde{\mathbf{H}}^{(i)}(\mathbf{q}^{(i)})\ddot{\tilde{\mathbf{x}}}^{(i)} + \tilde{\mathbf{C}}^{(i)}(\mathbf{q}^{(i)},\dot{\mathbf{q}}^{(i)}) = \tilde{\mathbf{Q}}^{(i)} \qquad (1)$$

where the superscript "i" corresponds to the i-th manipulator, $\mathbf{q}^{(i)}$ is the vector of generalized coordinates (consisting of joint angles and displacements), and $\tilde{\mathbf{x}}^{(i)}$ describes the output coordinates. Note that $\tilde{\mathbf{C}}^{(i)}$ contains all the gravity and nonlinear velocity terms, whereas in a microgravity environment the gravity terms are practically zero [13].

Assuming that each manipulator has six DOF, and using a square Jacobian $\mathbf{J}_C^{(i)}$, the output speeds ($\dot{\tilde{\mathbf{x}}}^{(i)}$) are computed in terms of the joint rates ($\dot{\mathbf{q}}^{(i)}$) as

$$\dot{\tilde{\mathbf{x}}}^{(i)} = \mathbf{J}_C^{(i)}\,\dot{\mathbf{q}}^{(i)} \qquad (2)$$

$\tilde{\mathbf{x}}^{(i)} = \left(\mathbf{x}_E^{(i)T}, \delta_E^{(i)T}\right)^T$ where $\mathbf{x}_E^{(i)}$ describes the i-th end-effector position, and $\delta_E^{(i)}$ is a set of Euler angles which describes the i-th end-effector orientation.

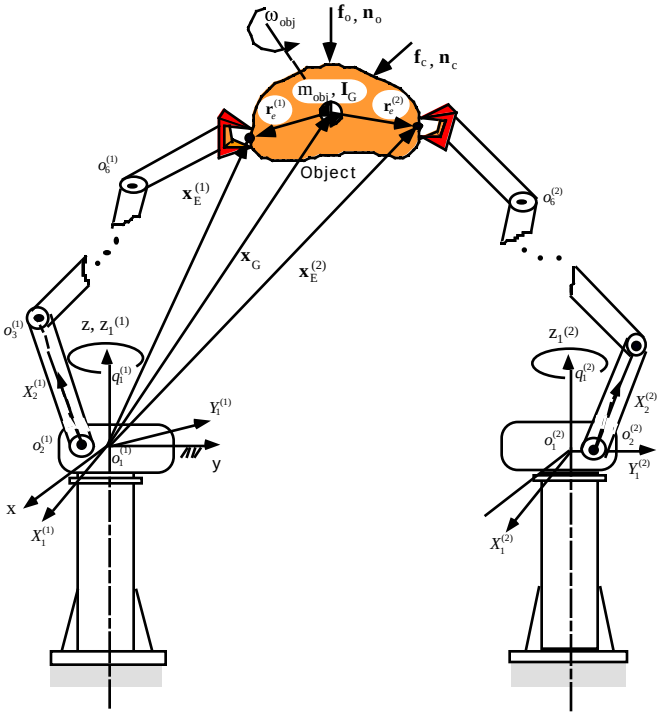

Fig. 2: Two robotic arms performing a cooperative manipulation task.

The vector of generalized forces in the task space, $\tilde{\mathbf{Q}}^{(i)}$, can be written as

$$\tilde{\mathbf{Q}}^{(i)} = \tilde{\mathbf{Q}}_{app}^{(i)} + \tilde{\mathbf{Q}}_{react}^{(i)} \qquad (3a)$$

where $\tilde{\mathbf{Q}}_{react}^{(i)}$ is the reaction load on the end-effector, and $\tilde{\mathbf{Q}}_{app}^{(i)}$ is the applied controlling force which is divided into two parts, *motion-concerned* and *force-concerned* as

$$\tilde{\mathbf{Q}}_{app}^{(i)} = \tilde{\mathbf{Q}}_{m}^{(i)} + \tilde{\mathbf{Q}}_{f}^{(i)} \qquad (3b)$$

where $\tilde{\mathbf{Q}}_{m}^{(i)}$ is the applied control force causing motion of the end-effector, while $\mathbf{Q}_{f}^{(i)}$ is the required force to be applied on the manipulated object by the end-effector. To obtain proper expressions for these terms, the equations of motion for the manipulated object are considered next.

(b) Object Dynamics. The equations of motion for a rigid object can be written as

$$\mathbf{M}\ddot{\mathbf{x}} + \mathbf{F}_\omega = \mathbf{F}_c + \mathbf{F}_o + \mathbf{G}\mathbf{F}_e \tag{4a}$$

where $\mathbf{M}$ is the mass matrix, $\mathbf{x} = (\mathbf{x}_G^T, \delta_{obj}^T)^T$ describes the position of the object center of mass $\mathbf{x}_G$ and the object orientation described by Euler angles δ_{obj}, $\mathbf{F}_\omega$ is a vector of nonlinear velocity terms, $\mathbf{F}_c$ describes the contact forces/moments, $\mathbf{F}_o$ are external forces/torques (other than contact and end-effector ones), $\mathbf{F}_e$ is a $6n\times1$ vector which contains all end-effector forces/torques applied on the object ($\mathbf{F}_e^{(i)}$ is a 6×1 vector corresponding to the i-th end-effector), and the matrix $\mathbf{G}$ which will be referred to as the *grasp matrix*, is obtained as [12]

$$\mathbf{G} = \begin{bmatrix} \mathbf{1}_{3\times3} & \mathbf{0}_{3\times3} & \cdots & \mathbf{1}_{3\times3} & \mathbf{0}_{3\times3} \\ \mathbf{S}_{obj}^T[\mathbf{r}_e^{(1)}]_{3\times3}^\times & \mathbf{S}_{obj}^T & \cdots & \mathbf{S}_{obj}^T[\mathbf{r}_e^{(n)}]_{3\times3}^\times & \mathbf{S}_{obj}^T \end{bmatrix}_{6\times6n} \tag{4b}$$

where $\mathbf{1}$ and $\mathbf{0}$ denote the identity and zero matrices, respectively. The matrix $\mathbf{S}_{obj}$ is introduced in Eq. (7), and $\mathbf{r}_e^{(i)}$ is the position vector of the i-th end-effector with respect to the object center of mass, see Fig. 2. Note that due to its formulation, the MIC takes into account the potentially large object or payload inertia forces. Next, using the system dynamics model and the object dynamics equations, the MIC law is developed.

(c) The MIC General Formulation. A desired impedance relationship for the object motion is chosen as

$$\mathbf{M}_{des}\ddot{\mathbf{e}} + \mathbf{k}_d\dot{\mathbf{e}} + \mathbf{k}_p\mathbf{e} = -\mathbf{F}_c \tag{5}$$

where $\mathbf{M}_{des}$ is the object desired mass matrix, $\mathbf{e} = \mathbf{x}_{des} - \mathbf{x}$ is the object position/orientation error vector, and $\mathbf{k}_p$ and $\mathbf{k}_d$ are gain matrices, usually diagonal. Comparing Eq. (5) to Eq. (4), it can be seen that the desired impedance behavior can be obtained if

$$\begin{aligned}\mathbf{G}\mathbf{F}_{e_{req}} = \mathbf{M}\mathbf{M}_{des}^{-1}\left(\mathbf{M}_{des}\ddot{\mathbf{x}}_{des} + \mathbf{k}_d\dot{\mathbf{e}} + \mathbf{k}_p\mathbf{e} + \mathbf{F}_c\right) + \\ \mathbf{F}_\omega - \left(\mathbf{F}_c + \mathbf{F}_o\right)\end{aligned} \tag{6}$$

provided that the matrix $\mathbf{S}_{obj}$ which relates the object angular velocity, ω_{obj}, and the Euler rates, δ_{obj}, as [14]

$$\omega_{obj} = \mathbf{S}_{obj}\dot{\delta}_{obj} \tag{7}$$

is not singular. Clearly, this depends on the Euler angles definition. Eq. (6) can be solved for the required end-effector forces to obtain the minimum norm solution

$$\begin{aligned}\mathbf{F}_{e_{req}} = \mathbf{G}^\#\{\mathbf{M}\mathbf{M}_{des}^{-1}\left(\mathbf{M}_{des}\ddot{\mathbf{x}}_{des} + \mathbf{k}_d\dot{\mathbf{e}} + \mathbf{k}_p\mathbf{e} + \mathbf{F}_c\right) + \\ \mathbf{F}_\omega - \left(\mathbf{F}_c + \mathbf{F}_o\right)\}\end{aligned} \tag{8}$$

where $\mathbf{G}^\#$ is the weighted pseudoinverse of the grasp matrix $\mathbf{G}$. The matrix $\mathbf{G}^\#$ is of full-rank provided that $\mathbf{S}_{obj}$ is not singular, and is defined as

$$\mathbf{G}^\# = \mathbf{W}^{-1}\mathbf{G}^T\left(\mathbf{G}\mathbf{W}^{-1}\mathbf{G}^T\right)^{-1} \tag{9}$$

where $\mathbf{W}$ is a task weighting matrix which allows for relative weighing of linear and angular variables. Assuming that $\mathbf{F}_o$, the object mass, and geometric properties are known, computation of $\mathbf{F}_{e_{req}}$ requires knowing the value of the contact force, $\mathbf{F}_c$. Since it is not possible, in general, to measure this force, it must be estimated. Therefore, Eq. (8) is written as

$$\begin{aligned}\mathbf{F}_{e_{req}} = \mathbf{G}^\#\{\mathbf{M}\mathbf{M}_{des}^{-1}\left(\mathbf{M}_{des}\ddot{\mathbf{x}}_{des} + \mathbf{k}_d\dot{\mathbf{e}} + \mathbf{k}_p\mathbf{e} + \hat{\mathbf{F}}_c\right) + \\ \mathbf{F}_\omega - \left(\hat{\mathbf{F}}_c + \mathbf{F}_o\right)\}\end{aligned} \tag{10}$$

where $\hat{\mathbf{F}}_c$ is the estimated value of the contact force $\mathbf{F}_c$. Depending on the grasp condition, if it is required to apply additional internal forces and moments on the object, $\mathbf{F}_{\text{int}}$, then Eq. (10) can be modified to

$$\begin{aligned}\mathbf{F}_{e_{req}} = \mathbf{G}^\#\{\mathbf{M}\mathbf{M}_{des}^{-1}\left(\mathbf{M}_{des}\ddot{\mathbf{x}}_{des} + \mathbf{k}_d\dot{\mathbf{e}} + \mathbf{k}_p\mathbf{e} + \hat{\mathbf{F}}_c\right) + \\ \mathbf{F}_\omega - \left(\hat{\mathbf{F}}_c + \mathbf{F}_o\right)\} + \left(\mathbf{1} - \mathbf{G}^\#\mathbf{G}\right)\mathbf{F}_{\text{int}}\end{aligned} \tag{11}$$

where $\mathbf{1}$ is a $6n\times6n$ identity matrix. Note that $\mathbf{F}_{\text{int}}$ does not affect the object motion, since the added term is in the null space of the grasp matrix $\mathbf{G}$.

According to the definition of $\mathbf{F}_e$, the force which has to be supplied by the i-th end-effector, $\mathbf{F}_{e_{req}}^{(i)}$, can be directly obtained from $\mathbf{F}_{e_{req}}$. This yields the force-concerned part of the applied controlling force, $\tilde{\mathbf{Q}}_f^{(i)}$, see Eq. (3), as

$$\tilde{\mathbf{Q}}_f^{(i)} = \mathbf{F}_{e_{req}}^{(i)} \tag{12}$$

Note that $\tilde{\mathbf{Q}}_f^{(i)}$ is virtually canceled by the reaction load on each end-effector. On the other hand, the reaction load is

$$\tilde{\mathbf{Q}}_{react}^{(i)} = -\mathbf{F}_e^{(i)} \tag{13a}$$

where

$$\mathbf{F}_e = \mathbf{G}^\#\left[\mathbf{M}\ddot{\mathbf{x}} + \mathbf{F}_\omega - (\mathbf{F}_c + \mathbf{F}_o)\right] + \left(\mathbf{1} - \mathbf{G}^\#\mathbf{G}\right)\mathbf{F}_{\text{int}} \tag{13b}$$

Next, we have to obtain a proper expression for the motion-concerned part of the applied controlling force, $\mathbf{Q}_m^{(i)}$.

As discussed earlier, through the MIC algorithm the same impedance law is imposed on the behavior of both the end-effector(s) and the manipulated object. Therefore, similar to Eq. (5), the impedance law for the i-th end-effector can be written as

$$\mathbf{M}_{des}\ddot{\tilde{\mathbf{e}}}^{(i)} + \mathbf{k}_d\dot{\tilde{\mathbf{e}}}^{(i)} + \mathbf{k}_p\tilde{\mathbf{e}}^{(i)} = -\mathbf{F}_c \tag{14}$$

where $\tilde{\mathbf{e}}^{(i)} = \tilde{\mathbf{x}}_{des}^{(i)} - \tilde{\mathbf{x}}^{(i)}$ is the i-th end-effector position/orientation error vector. Then, $\tilde{\mathbf{Q}}_m^{(i)}$ can be obtained similar to the above derivation for $\tilde{\mathbf{Q}}_f^{(i)}$, as

$$\begin{aligned}\tilde{\mathbf{Q}}_m^{(i)} = \tilde{\mathbf{H}}^{(i)}(\mathbf{q}^{(i)})\mathbf{M}_{des}^{-1}\left[\mathbf{M}_{des}\ddot{\tilde{\mathbf{x}}}_{des}^{(i)} + \mathbf{k}_d\dot{\tilde{\mathbf{e}}}^{(i)} + \mathbf{k}_p\tilde{\mathbf{e}}^{(i)} + \mathbf{F}_c\right] + \\ \tilde{\mathbf{C}}^{(i)}(\mathbf{q}^{(i)}, \dot{\mathbf{q}}^{(i)})\end{aligned} \tag{15a}$$

or, after substituting the estimated value for the contact force

$$\begin{aligned}\tilde{\mathbf{Q}}_m^{(i)} = \tilde{\mathbf{H}}^{(i)}(\mathbf{q}^{(i)})\mathbf{M}_{des}^{-1}\left[\mathbf{M}_{des}\ddot{\tilde{\mathbf{x}}}_{des}^{(i)} + \mathbf{k}_d\dot{\tilde{\mathbf{e}}}^{(i)} + \mathbf{k}_p\tilde{\mathbf{e}}^{(i)} + \hat{\mathbf{F}}_c\right] + \\ \tilde{\mathbf{C}}^{(i)}(\mathbf{q}^{(i)}, \dot{\mathbf{q}}^{(i)})\end{aligned} \tag{15b}$$

Substituting Eqs. (12), and (15) into Eq. (3b), the applied controlling force is computed.

Note that OIC enforces an impedance law only on the object motion, while MIC enforces an impedance law on both the manipulator end-effector(s), and the manipulated object. This major difference between the MIC and OIC allows for proper trajectory planning of the end-effector(s),

based on the desired trajectory for the object, and the grasp condition. The desired trajectory for the i-th end-effector motion, $\tilde{\mathbf{x}}_{des}^{(i)}$, is defined based on the desired trajectory for the object motion, the object geometry, and the grasp condition. In other words, based on the *grasp constraints* defined as

$$\mathbf{g}^{(i)}(\mathbf{x}_{des}, \tilde{\mathbf{x}}_{des}^{(i)}) = \mathbf{0} \qquad i = 1, \cdots, n \tag{16}$$

and the object desired trajectory, $\mathbf{x}_{des}$, the desired end-effectors trajectories and corresponding time derivatives can be determined. Therefore, satisfaction of the grasp constraints is guaranteed, as well as an impedance controlled motion of all participating end-effectors. In the case of a redundant system, the end-effector(s) trajectory can be planned so as to optimize performance.

(d) Error Analysis. It can be shown that substituting Eqs. (12), (13), and (15) into Eq. (3), and then the result into Eq. (1), yields

$$\begin{aligned} &\mathbf{M}_{des}\ddot{\tilde{\mathbf{e}}}^{(i)} + \mathbf{k}_d\dot{\tilde{\mathbf{e}}}^{(i)} + \mathbf{k}_p\tilde{\mathbf{e}}^{(i)} + \hat{\mathbf{F}}_c = \mathbf{0} \qquad i = 1, \cdots, n \\ &\mathbf{M}_{des}\ddot{\mathbf{e}} + \mathbf{k}_d\dot{\mathbf{e}} + \mathbf{k}_p\mathbf{e} + \hat{\mathbf{F}}_c = \mathbf{0} \end{aligned} \tag{17}$$

For more details see [12], or follow a similar derivation for space robotic systems in [11]. The above equation means that all participating manipulators and the manipulated object exhibit the same designated impedance behavior. Therefore, the MIC algorithm imposes a consistent motion of all parts of the system. In an ideal case, this results in a harmonic motion of different parts of the system like the motion of a multi-DOF system in its natural mode shapes. Note that the MIC approach permits choosing different impedance parameters for the object dynamical behavior and the end-effectors (by selecting $\mathbf{M}_{des}$, $\mathbf{k}_d$, and $\mathbf{k}_p$ in Eq. (14) different from those of Eq. (5)). However, physical intuition as well as simulation analyses indicate that the best results are achieved by choosing the same parameters. This is due to the fact that enforcing the same pre-set impedance on different parts of the system results in an accordant motion throughout the system while executing a manipulation task. A harmonious motion of the end-effectors and of the manipulated object is ensured via the same error dynamics as described by Eq. (17).

(e) Contact Force Estimation. Computation of $\mathbf{F}_{e_{req}}$ requires knowing the value of the contact force, $\mathbf{F}_c$. In general, this has to be estimated which is discussed below. To compute the contact force, Eq. (4) can be rewritten as

$$\mathbf{F}_c = \mathbf{M}\ddot{\mathbf{x}} + \mathbf{F}_\omega - \mathbf{F}_o - \mathbf{G}\mathbf{F}_e \tag{18}$$

It is assumed that $\mathbf{F}_o$, the object mass, and the geometric parameters are known. If the end-effectors are equipped with force sensors, $\mathbf{F}_e$ can be measured and substituted into this equation. Also, based on measurements of object motion, $\mathbf{F}_\omega$ can be computed and substituted into Eq. (18). However, to evaluate the contact force, the object acceleration must be known also. Since this is not usually available, it can be approximated through a numerical estimation procedure. In the OIC implementation, either the desired acceleration, or the last *commanded acceleration* which is defined as

$$\ddot{\mathbf{x}}_{cmd} = \mathbf{M}_{des}^{-1}\left(\mathbf{M}_{des}\ddot{\mathbf{x}}_{des} + \mathbf{k}_d\dot{\mathbf{e}} + \mathbf{k}_p\mathbf{e} + \hat{\mathbf{F}}_c\right) \tag{19}$$

are used. Although both of these two approximations yield acceptable experimental results, it has been indicated that a more sophisticated procedure would improve performance [12]. In fact, since there may be a considerable difference between $\ddot{\mathbf{x}}$ and $\ddot{\mathbf{x}}_{des}$, using $\ddot{\mathbf{x}}_{des}$ will not yield reliable results especially after contact. On the other hand, using Eq. (19) may result in a poor approximation because of sudden variations in contact forces.

Here, the suggestion is to use finite difference approximation as

$$\dot{\hat{\mathbf{x}}} = \frac{\dot{\mathbf{x}}_t - \dot{\mathbf{x}}_{t-\Delta t}}{\Delta t} \quad \text{or} \quad \ddot{\hat{\mathbf{x}}} = \frac{\mathbf{x}_t - 2\mathbf{x}_{t-\Delta t} + \mathbf{x}_{t-2\Delta t}}{(\Delta t)^2} \tag{20}$$

where Δt is the time step used in the estimation procedure. In a noisy environment, higher order finite difference estimates may be needed. Note that due to practical reasons (i.e. time requirements for measurements and corresponding calculations), Δt can not be infinitesimally close to zero. At sufficiently high sampling rates, this does not introduce a significant error, even during contact. Substituting Eq. (20) for acceleration, the contact force can be estimated based on Eq. (18) as

$$\hat{\mathbf{F}}_c = \mathbf{M}\ddot{\hat{\mathbf{x}}} + \mathbf{F}_\omega - \mathbf{F}_o - \mathbf{G}\mathbf{F}_e \tag{21}$$

IV. Case Study: A Comparative Analysis.

The single robotic arm manipulating an object, depicted in Figure 1, is used here to compare the performance of the MIC and OIC algorithms. As shown in [12], the sum of the roots of characteristic equation for the system under the MIC and OIC laws is obtained as

$$\sum_{MIC} s_i = \frac{-\left(\hat{m}_1 m_2 m_3 k_d + m_{des}(m_1 + m_2)m_3 b_1 + m_{des}(m_2 + m_3)m_1 b_2\right)}{m_{des} m_1 m_2 m_3}$$

$$\sum_{OIC} s_i = \frac{-\left((m_1 + m_2)m_3 b_1 + (m_2 + m_3)m_1 b_2\right)}{m_1 m_2 m_3}$$

As it is seen, the latter is a function of system parameters only, and is mostly affected by damping characteristics of the system; the controller parameters do not affect the sum of the roots for the OIC algorithm. However, it is seen that for the MIC, the summation is also a function of k_d and m_{des}, besides system parameters, which permits easier pole placement.

For a rigid manipulator and object, both algorithms yield the same closed-loop transfer functions, [12]. In the presence of system flexibility, the root loci for the MIC and OIC algorithms, as a function of the object stiffness (k_2) for various damping factors (b_2), reveal that for a relatively well-damped object both algorithms are stable, whether or not the object is in contact with an obstacle, [12]. However, for an object with light damping, the OIC algorithm can become unstable if there is no contact. Figure 3 shows a set of typical root loci plots where the system parameters are the same as those introduced in the following simulation part (except for b_2 =10). Note that contact between the object and

an obstacle adds a feedback effect to the system, and so its dynamic behavior changes.

It can be shown that choosing larger gains does not result in a stable system under the OIC law. However, a larger desired mass ($\mathbf{M}_{des}$) has a positive effect on the stability of this algorithm, though it results in a sluggish performance. For an undamped object, i.e. $b_2 = 0$, it is observed that the MIC algorithm is stable (whether or not the object is in contact with the obstacle), while the OIC becomes unstable. In this case, choosing a larger value for the desired mass or a larger damping gain does not result in a stable system. It can be concluded that with respect to system stability, the MIC algorithm exhibits better characteristics than the OIC.

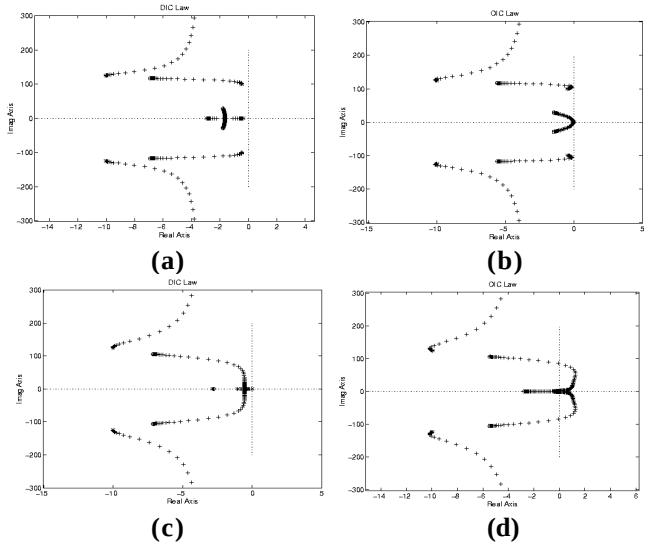

Fig. 3: Root loci for $b_2 = 10.0$. (a) MIC (contact), (b) OIC (contact), (c) MIC (free space), (d) OIC (free space). The OIC can result in an unstable system.

Simulation Results. The performance of a system of two cooperating two-link manipulators, in which a Remote Centre Compliance is attached to the second end-effector, was presented in [11]. It was shown by simulation that even in the presence of flexibility and impact forces, the MIC yields a smooth and stable performance. Here, for the purpose of comparison, the system depicted in Fig. 1 is simulated under the MIC and OIC laws, where the system parameters are chosen so that stability is ensured in both *no contact* and *in contact* phases. To focus on the structural behavior of these algorithms, it is assumed that the exact value of the contact force, f_c, is available to the controllers. The system mass parameters are chosen as $m_1 = 100\,kg$, $m_2 = 20.0\ kg$, and $m_3 = 10.0\ kg$. Assuming a relatively high fundamental frequency of 20 Hz, and a logarithmic decrement δ of 0.2 for the manipulator, $k_1 = 2.6 \times 10^5\ N/m$ and $b_1 = 325\,kg/\sec$ are obtained, where $k_2 = 2.0 \times 10^4\ N/m$ and $b_2 = 100.0\,kg/\sec$ are selected. The controller parameters are chosen as

$$m_{des} = 100.0,\ k_p = 100.0,\ k_d = 700.0$$

To approximate actuator dynamics, the input force F_1 is filtered by a second-order Butterworth *low-pass filter*, as

$$\frac{F_{1_{filtered}}}{F_1} = \frac{\omega_0^{\,2}}{s^2 + \sqrt{2}\omega_0 s + \omega_0^{\,2}} \tag{22}$$

where ω_0 is chosen equal to 30 rad/sec. The obstacle is at $x_w = 0.7m$, and the contact force is computed as

$$\begin{array}{l} if \quad x_3 > x_w \quad f_c = k_w(x_w - x_3) \\ else \quad f_c = 0.0 \end{array} \tag{23}$$

where $k_w = 1e5\,N/m$. The desired trajectory for the object is defined as $x_{3\,des} = 1 - e^{-t}$, and the initial conditions are

$$(x_1,\ x_2,\ x_3,\ \dot{x}_1,\ \dot{x}_2,\ \dot{x}_3)^T = (-0.2, -0.1, 0.01, 0,\ 0, 0)^T \quad (m, m/s)$$

and it is assumed that each spring is initially free of tension or compression.

Figure 4 compares the simulated performance of the MIC and OIC algorithms during the free motion and contact phase. Root locus analysis shows that both OIC and MIC are stable in both the "no contact" and "in contact" phases. As shown in Figure 4, under the OIC law the system oscillates reaching a limit-cycle, while the MIC algorithm yields a good response, and the object comes into contact with the obstacle at $t \approx 2.0$ sec.

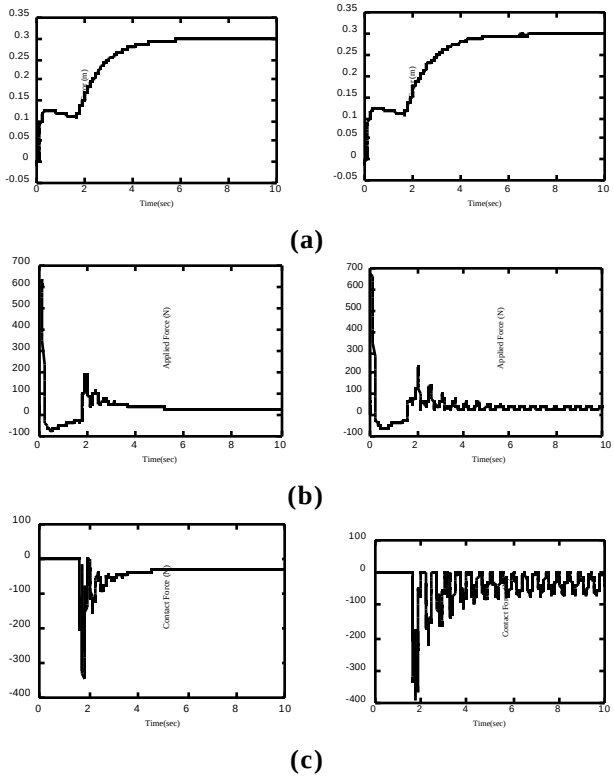

Fig. 4: Performance of the MIC (left) compared to the OIC (right), (a) Object tracking error, (b) The applied controlling force, (c) The contact force.

Applying the OIC law results in an oscillatory error, see Figure 4a. This is due to the presence of flexibility between

the end-effector and the object center of mass as its reference point in the control law. Note that the OIC is formulated at the object level, with no feedback of the end-effector's motion. The sustained oscillatory error demands an oscillating input force (Figure 4b), which in turn results in a persistent impact force due to the contact with the obstacle (Figure 4c).

It can be shown that by choosing larger damping gains, k_d, the resulting oscillations for the OIC do not disappear, though the amplitudes may decrease. By choosing larger k_p's, the oscillations get worse (the amplitudes increase), while the MIC still results in a good response. The effect of actuator saturation limits on the performance of both algorithms was also studied. It was shown that in almost all cases, the system oscillates under the OIC law, while the MIC always results in a smooth stop of the object at the obstacle, [12]. Based on our simulation results, it is concluded that the new MIC algorithm yields improved performance over the OIC.

V. Conclusions

In this paper, a new algorithm called Multiple Impedance Control (MIC) was developed for cooperative object manipulation. The MIC enforces a designated impedance on cooperating manipulators *and* on the manipulated object, which results in a consistent motion of all members of a system besides satisfying the grasp constraint. Similar to the standard impedance control, one of the benefits of this algorithm is the ability to perform both free motions and contact tasks without switching the control modes. In addition, an object's inertia effects are compensated in the impedance law, and at the same time the end-effector(s) tracking errors are controlled. Error analysis shows that under the MIC law all participating manipulators, and the manipulated object exhibit the same designated impedance behavior. An estimation procedure for contact force determination was given which results in a good approximation, even during contact. A linear model of an object manipulation task by a single manipulator was considered to present a comparative analysis between the MIC and Object Impedance Control (OIC). It was shown that even in the presence of flexibility and contact forces due to the existence of an obstacle, the performance of the MIC algorithm is reasonably good.

Acknowledgments

The support of this work by the Natural Sciences and Engineering Council of Canada (NSERC) is acknowledged.

References

[1] Raibert, M. H. and Craig, J. J., "Hybrid Position/Force Control of Manipulators," *ASME Journal of Dynamic Systems, Measurement & Control*, Vol. 126, June 1981, pp. 126-133.

[2] Khatib, O., "A Unified Approach for Motion and Force Control of Robot Manipulators: The Operational Space Formulation," *IEEE Journal of Robotics and Automation*, Vol. RA-3, No. 1, February 1987, pp. 43-53.

[3] Schutter, J.D., et al., "Invariant Hybrid Force/Position Control of a Velocity Controlled Robot with Compliant End Effector Using Modal Decoupling," *Int. J. of Robotics Research*, Vol. 16, No. 3, June 1997, pp. 340-356.

[4] Nakamura, Y., Nagai, K., and Yoshikawa, T., "Mechanics of Coordinative Manipulation by Multiple Robotic Mechanisms," *Proc. of IEEE Int. Conf. on Robotics and Automation*, April 1987, pp. 991-998.

[5] Hogan, N., "Impedance Control: An Approach to Manipulation -A Three Part Paper," *ASME Journal of Dynamic Systems, Measurement, and Control*, Vol. 107, March 1985, pp. 1-24.

[6] Goldenberg, A. A., "Implementation of Force and Impedance Control in Robot Manipulators," in *Proc. of the IEEE Int. Conf. on Robotics and Automation*, Philadelphia, Pennsylvania, April 1988, pp. 1626-1632.

[7] Pelletier, M. and Daneshmend, L.K., "Automatics Synthesis of Robot Compliant Motions in Dynamic Environments", *Int. J. of Robotics Research, Vol. 16, No. 6, December 1997, pp. 730-748.*

[8] Seraji, H. and Colbaugh, R., "Force Tracking in Impedance Control," *Proc. of IEEE Int. Conf. on Robotics and Automation*, Atlanta, Georgia, May 1993, pp. 499-506.

[9] Schneider, S. A. and Cannon, R. H., "Object Impedance Control for Cooperative Manipulation: Theory and Experimental Results," *IEEE Transactions on Robotics and Automation*, Vol. 8, No. 3, June 1992, pp. 383-394.

[10] Meer, D. W. and Rock, S. M., "Coupled-System Stability of Flexible-Object Impedance Control," in *Proc. of the IEEE Int. Conf. on Robotics and Automation*, Nagoya, Japan, May 1995, pp. 1839-1845.

[11] Moosavian, S. Ali A. and Papadopoulos, E., "On the Control of Space Free-Flyers Using Multiple Impedance Control," *Proc. IEEE Int. Conf. on Robots and Automation*, Albuquerque, NM, USA, April 21-27, 1997.

[12] Moosavian, S. Ali A., "Dynamics and Control of Free-Flying Manipulators Capturing Space Objects," *Ph.D. thesis*, McGill University, Montreal, Canada, June 1996.

[13] Papadopoulos, E. and Moosavian, S. Ali A., "Dynamics & Control of Space Free-Flyers with Multiple Arms," *Journal of Advanced Robotics*, Vol. 9, No. 6, 1995, pp. 603-624.

[14] Meirovitch, L., *Methods of Analytical Dynamics*, McGraw-Hill, 1970.